Analytical solution to the optical transfer function of a scattering medium with large particles

Eleanor P. Zege and Alexander A. Kokhanovsky

A new analytical expression for the optical transfer function of multiple-scattering media such as clouds, mists, and dust aerosols is given in terms of their microphysical characteristics. The geometrical optics approximation is used to find local optical parameters of a scattering medium, including the simple approximation of the phase function, which is the key to the solution of the problem considered here. The optical transfer function is taken within a small-angle approximation of the radiative transfer theory. A comparison with Monte Carlo data shows a fairly satisfactory accuracy of our analytic formulas.

Key words: Radiative transfer theory, small-angle approximation optical transfer function, geometrical optics.

1. Introduction

It is the optical transfer function (OTF) that is the basic characteristic responsible for image transfer through a scattering medium (e.g., atmospheric aerosols, clouds, and fogs).[1–4] The OTF of the scattering medium depends on the medium's microstructure and thickness. When the effect of the microstructure on image-transfer characteristics is studied, the Mie calculations are used to obtain single-scattering characteristics, and then the Monte Carlo simulations provide the OTF's.[4,5] It is a direct and reliable technique, but how cumbersome and time consuming it is! Moreover, it is not exactly what we need for design estimations.

The phase functions of real scattering media (aerosols, clouds, mists, sea water, etc.) are highly extended, and the scattering is predominantly in the forward direction. That is why the small-angle approximation (SAA)[1,2] can be used to rescue the situation, and it provides an elegant OTF solution for this particular case. But the strongly extended phase functions are applicable only to scattering by large particles.[6–10] In addition the Mie calculations become more cumbersome the larger the particles. The geometrical optics approximation[7,10] is an adequate tool to use for the study of large particles.

The authors are with the Institute of Physics, Prospect F. Scoryna 70, Minsk 220602, Belarus.

Received 19 April 1993; revision received 1 January 1994.
0003-6935/94/276547-08$06.00/0.

In this paper we consider imaging through a scattering medium that is a polydispersion of large spherical particles where the diffraction parameter $\rho = ka \gg 1$, $k = 2\pi/\lambda$, λ is the wavelength, and a is the particle radius. Let $f(a)$ be the particle-size distribution (PSD), and let $m = n - i\chi$ be the complex refractive index of the particle. The optical parameters of the scattering medium are the extinction ε and scattering σ coefficients and the phase function $P(\theta)$ (θ is the scattering angle). Geometrical optics solutions for ε, σ, and $P(\theta)$ are known.[7–10]

Essentially we have simplified the known geometrical optics solution for $P(\theta)$ (see Appendix A). Combining the obtained formula with the SAA solution for the OTF provides the desired analytical solution, which directly relates the OTF of the medium to its particle characteristics, m and $f(a)$. The results of the combined Mie and Monte Carlo computations[5] were used to test our simple result, and a high accuracy for fog and clouds has been obtained.

The solution obtained provides an ample scope for the study of the effect of the microstructure on the transfer characteristics of clouds and fog.

2. Theory

For scattering media with a moderate optical thickness τ and an extended phase function, the OTF $S(\omega^*)$ can be estimated with the SAA[1,11]:

$$S(\omega^*) = \exp[-\tau + \eta(\omega^*)l], \tag{1}$$

$$\tau = \varepsilon l, \qquad \eta(\omega^*) = \int_0^1 \sigma(\omega^* y)\mathrm{d}y,$$

$$\sigma(\omega^* y) = \frac{1}{2}\int_0^\infty \sigma(\theta) J_0(\omega^* y\theta)\theta \mathrm{d}\theta. \tag{2}$$

Here $\omega^* = \nu l$ is the angular dimensionless frequency, ν is the spatial frequency, l is the observation depth, $J_0(\omega\theta)$ is the zero-order Bessel function, and $\sigma(\theta) = \sigma P(\theta)$. The OTF accuracy provided by Eq. (1) was discussed earlier,[5] and we too shall touch on this point in Section 4.

We consider only large particles, so we can use the reported geometrical optics result[7–10] for the extinction coefficient $\varepsilon = 2N\pi M_2$, where $M_2 = \int_0^\infty a^2 f(a)\mathrm{d}a$, and N is the particle number density. The simple formula for the function $\sigma(\theta)$ [Eqs. (A1) and (A10)] is derived in Appendix A. Taking into account Eq. (A10) we can rewrite the expression for $\eta(\omega^*)$ as

$$\eta(\omega^*) = \sum_{i=1}^{3} \eta_i(\omega^*), \tag{3}$$

$$\eta_i(\omega^*) = N\int_0^\infty \pi a^2 f(a)\eta_i(\omega^*, a)\mathrm{d}a, \tag{4}$$

$$\eta_i(\omega^*, a) = \frac{1}{2}\int_0^1 \mathrm{d}y \int_0^\infty \theta J_0(\omega^* y\theta) q_i(\theta)\mathrm{d}\theta, \tag{5}$$

where

$$q_1(\theta) = 4J_1^2(\theta\rho)/\theta^2, \qquad q_2(\theta) = \exp(-\alpha\theta),$$

$$q_3(\theta) = T(0)\exp(-\beta\theta^2 - c), \tag{6}$$

and where $c = 4\chi\rho$, and $T(0)$, α, and β depend only on n (see Appendix A). Substituting Eq. (6) in Eq. (5), we obtain

$$\eta_1(\omega^*, a) = \left[\frac{2}{\pi}\arccos b - \frac{2(2 + b^2)(1 - b^2)^{1/2}}{3\pi b}\right] \times U_+(1 - b) + \frac{4}{3\pi b}, \tag{7}$$

$$\eta_2(\omega^*, a) = \frac{1}{2\alpha^2[1 + (\omega^*/\alpha)^2]^{1/2}},$$

$$\eta_3(\omega^*, a) = \frac{T(0)e^{-c}}{4\omega^*}(\pi/\beta)^{1/2}\mathrm{erf}[\omega^*/2(\beta)^{1/2}]. \tag{8}$$

Here, $\mathrm{erf}(x) = 2/(\pi)^{1/2}\int_0^x \exp(-x^2)\mathrm{d}x$ is the probability integral, and $U_+(x)$ is the Heaviside unit function [$U_+(x) = 1$ at $x \geq 0$ and $U_+(x) = 0$ at $x < 0$], $b = \delta/a$, and $\delta = \omega^*/2k$. The following simple approximation of Eq. (7) can be used (the error will be $<2\%$):

$$\eta_1(\omega^*, a) = \begin{cases} 1 - \dfrac{2b}{\pi}\left(1 - \dfrac{b^2}{12}\right), & b < 1 \\ \dfrac{4}{3\pi b}, & b \geq 1 \end{cases} \tag{9}$$

Substitution of Eqs. (8) and (9) into Eq. (4) gives

$$\eta_1(\omega^*) = \frac{4N}{3\pi\delta}\int_0^\delta \pi a^3 f(a)\mathrm{d}a + N\int_\delta^\infty \pi a^2 f(a) \times \left[1 - \frac{2\delta}{\pi a}\left(1 - \frac{\delta^2}{12a^2}\right)\right]\mathrm{d}a, \tag{10}$$

$$\eta_2(\omega^*) = \frac{\pi N M_2}{2\alpha^2[1 + (\omega^*/\alpha)^2]^{1/2}}, \tag{11}$$

$$\eta_3(\omega^*) = \frac{T(0)N\pi M_2^*}{4\omega^*}(\pi/\beta)^{1/2}\mathrm{erf}[\omega^*/2(\beta)^{1/2}], \tag{12}$$

where

$$M_j = \int_0^\infty a^j f(a)\mathrm{d}a, \qquad M_j^* = \int_0^\infty a^j e^{-c} f(a)\mathrm{d}a. \tag{13}$$

The function $\eta_1(\omega^*)$ can be represented in the more convenient form of

$$\eta_1(\omega^*) = N\left[\pi(M_2 - \overline{M}_2) - 2\delta(M_1 - \overline{M}_1) + \frac{\delta^3}{6}(M_{-1} - \overline{M}_{-1}) + \frac{4}{3\delta}\overline{M}_3\right], \tag{14}$$

where $\overline{M}_j = \int_0^\delta a^j f(a)\mathrm{d}a$. As follows from Eq. (14) at $\omega^* \to 0(\delta \to 0)$, the value of

$$\eta_1 = N\pi M_2(1 - \omega^*/\pi\rho_{21}), \qquad \rho_{21} = kM_2/M_1, \tag{15}$$

while at $\omega^* \to \infty(\delta \to \infty)$

$$\eta_1 = 8kNM_3/3\omega^*. \tag{16}$$

From Eqs. (11) and (12) we obtain at $\omega^* \to \infty$

$$\eta_2 = \frac{N\pi M_2}{2\alpha\omega^*}, \qquad \eta_3 = \frac{N\pi M_2^* T(0)}{4\omega^*}(\pi/\beta)^{1/2}, \tag{17}$$

and at $\omega^* \to 0$

$$\eta_2 = \frac{N\pi M_2}{2\alpha^2}\left[1 - \frac{1}{2}\left(\frac{\omega^*}{\alpha}\right)^2\right],$$

$$\eta_3 = \frac{\pi N M_2^* T(0)}{4\beta}\left[1 - \frac{1}{12\beta}(\omega^*)^2\right]. \tag{18}$$

As seen from Eqs. (16) and (17), at $\omega^* \gg 1$, the ratios η_2/η_1 and η_3/η_1 are independent of ω^* and are of the order of the small value $\rho_{32}^{-1} = (ka_{32})^{-1}$ and $a_{32} = M_3/M_2$. For instance, for water droplets in the visible spectrum ($\chi = 0, M_2^* = M_2$) with regard to the data of Table 1 and formulas (16) and (17), we have $\eta_2/\eta_1 = 0.2/\rho_{32}$ and $\eta_3/\eta_1 = 3.7/\rho_{32}$. So, the larger the scatterers, the more decisive is the contribution of diffraction into $\eta(\omega^*)$ at high frequencies. For typical water clouds in the visible spectrum with $\rho_{32} \approx 60$, we obtain $\eta_2/\eta_1 = 0.003$ and $\eta_3/\eta_1 = 0.06$.

On the other hand, for nonabsorbing particles at the low frequencies ($\omega^* \ll 1$) the contributions of the geometrical optics terms and diffraction are comparable [see Eqs. (15) and (18)]. For strongly absorbing particles, when $M_2^* \to 0$ and $\eta_3(\omega^*) \to 0$ the contribution of the diffraction component is decisive at all frequencies (at $\omega^* \ll 1$ and $\eta_2/\eta_1 < 1/2\alpha^2$).

The analytical expressions can be obtained for the integrals of M_j and $\overline{M}_j$ in formulas (11), (12), and (14) for many typical PSD. Some of them are given in Table 1.

So, formulas (1)–(3), (11), (12), and (14) give us the desirable solution and directly relate the OTF to the particle characteristics $f(a)$ and m. Finally, from Eqs. (3), (11), (12), and (14) we have $\eta(\omega^*)$ [see Eq. (1)] in the form

$$\eta(\omega^*) = \left\{1 - Z_2 - \frac{2\delta a_{12}}{\pi}(1 - Z_1) + \frac{\delta^3}{6\pi} a_{-12}(1 - Z_{-1}) + \frac{4a_{32}}{3\pi\delta} Z_3 + \frac{1}{2\alpha^2[1 + (\omega^*/\alpha)^2]^{1/2}} + \frac{T(0)\gamma}{4\omega^*} \times (\pi/\beta)^{1/2}\mathrm{erf}[\omega^*/2(\beta)^{1/2}]\right\}\pi N M_2, \quad (19)$$

where (see Table 1)

$$a_{ij} = M_i/M_j, \qquad Z_j = \overline{M}_j/M_j, \qquad \gamma = M_2^*/M_2. \quad (20)$$

The first five terms in Eq. (19) originate from the Fraunhofer diffraction, and the sixth and seventh terms are due to the beams reflected from the surface and transmitted through the particle, respectively.

Note, that the M_j^* function in Eq. (20) can be given as

$$M_j^* = \sum_{k=0}^{\infty} \frac{(-1)^k(2\alpha)^k}{k!} M_{k+j}, \quad (21)$$

where $\alpha = 4\pi\chi/\lambda$. At $\alpha \ll 1$, from Eq. (21) we have

$$M_2^* = M_2(1 - 2\alpha a_{32}), \quad (22)$$

where $a_{32} = M_3/M_2$ is an effective radius of the polydispersion. As would be expected, at $\omega^* \to \infty$ from Eqs. (1) and (19), it follows that

$$S(\infty) = \exp(-\tau), \quad (23)$$

i.e., the OTF is determined only by the unscattered light.

At $\omega^* = 0$ a new and useful expression for the transmission coefficient can be obtained from Eqs. (1) and (19).

3. Transmission Coefficient under Normal Incidence

Really, the OTF at $\omega^* = 0$ gives the transmission coefficient of a layer[1] illuminated by a normally incident wide parallel beam $t(\tau, \mu_0 = 1)$ (μ_0 is the cosine of the angle between the incidence direction and the normal to the layer boundary), i.e., $t(\tau, \mu_0 = 1) = S(\omega^* = 0)$. From Eqs. (1) and (19) at

Table 1. PSD Moments M_j and Values of $Z_j = \overline{M}_j/M_j$ for the Most Frequently Used PSD's[a]

N	$f(a)$	M_j	Z_j
Gamma distribution[b]	$\left(\frac{\mu}{a_0}\right)^{\mu+1} \frac{a^\mu \exp(-\mu a/a_0)}{\Gamma(\mu + 1)}$	$\left(\frac{a_0}{\mu}\right)^j \frac{\Gamma(\mu + 1 + j)}{\Gamma(\mu + 1)}$	$P(\mu + 1 + j, \Delta)$, $\Delta = \frac{\mu\omega^*}{2\rho_0}$, $\rho_0 = ka_0$
Log-normal distribution[c]	$\frac{\exp(-0.5\sigma^{-2}\ln^2 a/a_m)}{a\sigma(2\pi)^{1/2}}$	$(a_m)^j \exp\left(\frac{\sigma^2 j^2}{2}\right)$	$\frac{1 + \mathrm{erf}(x)}{2}$, $x = \frac{1}{\sigma\sqrt{2}}\left\{\ln\frac{\omega^*}{2\rho^*} - j\sigma^2\right\}$, $\rho^* = \frac{2\pi a_m}{\lambda}$

[a] Here, $P(n, y)$ is the incomplete gamma function, $\Gamma(x)$ is the gamma function, and $\mathrm{erf}(x)$ is the probability integral.[12]
[b] Here, a_0 is the mode radius, and μ is the half-width parameter.
[c] Here, a_0 is the median radius and σ is the rms of the particle radius logarithm.

$\omega^* = 0$ we have

$$t(\tau, \mu_0 = 1) = \exp\left\{-\tau\left[\frac{1}{2} - \frac{1}{4\alpha^2} - \frac{M_2^*}{M_2}\frac{T(0)}{8\beta}\right]\right\}, \quad (24)$$

where the parameters α and β depend only on the real part of the refractive index (at $\chi \ll n$). Here $\tau = 2N\pi M_2 l$, which follows from the geometrical optics approximation.[7] It is a new expression for the transmission coefficient that relates it directly to the PSD moments and the value of m.

The following formula obtained through the SAA is known[1]:

$$t(\tau, \mu_0 = 1) = \exp[-\tau(1 - \Lambda^*)], \quad (25)$$

where $\Lambda^* = \Lambda F(\theta_0)$ is some efficient single-scattering albedo, $\Lambda = \sigma/\varepsilon$ is the true single-scattering albedo, and $F(\theta_0)$ is a part of the light flux singly scattered in the on-axis region $\theta < \theta_0$. Strictly speaking, the Λ^* value is not specified here: It depends on the choice of the value of θ_0, which differs in different works,[1,11] ranging from $\pi/6$ to $\pi/2$. Using formula (24), one can not only avoid this uncertainty, one can also relate the Λ^* value directly to the particle characteristics (n, χ, and PSD moments) by

$$\Lambda^* = \frac{1}{2}\left[1 + \frac{1}{2\alpha^2} + \frac{T(0)M_2^*}{4\beta M_2}\right]. \quad (26)$$

As follows from Eq. (24), in the two limiting cases ($\chi = 0$ and $\chi\rho \gg 1$), the transmission coefficient does not depend on χ, and for nonabsorbing media and we have

$$\Lambda^* = \frac{1}{2} + \frac{1}{4\alpha^2} + \frac{T(0)}{8\beta}. \quad (27)$$

While at strong absorption when $M_2^* \to 0$, we obtain

$$\Lambda^* = \frac{1}{2} + \frac{1}{4\alpha^2}, \quad (28)$$

where the term $1/4\alpha^2$ is small (see Table 2 in Appendix A). As follows from Eqs. (27) and (28) for water droplets in the visible spectrum ($m = 1.33$) $\Lambda^* = 0.94$, and for the dust aerosol in the visible ($m = 1.53 - 0.008i$ and $k\chi a_0 \gg 1$) $\Lambda^* = 0.54$.

The accuracy obtained with Eq. (24) is high. Comparison with different computation results has shown that at $\tau \le 7$ and $a_{32} \ge 10\lambda$ errors of the transparency estimations do not exceed 7%. Some illustrations will be given in Section 4.

4. Numerical Results and Comparison with Monte Carlo Simulations

Consider a scattering medium with a gamma PSD[6] (see Table 1). As follows from Eq. (19), with allowances made for the data of Table 1, $\eta(\omega)$ is of the form

$$\eta(\omega^*) = \Sigma\left\{1 + \frac{8\rho_{32}}{3\pi\omega^*}P(\mu + 4, \Delta) - P(\mu + 3, \Delta) - \frac{2\Delta}{\pi(\mu + 2)}[1 - P(\mu + 2, \Delta)] + \frac{\Delta^3}{6\pi\mu(\mu + 1)(\mu + 2)}[\mathbf{1 - P(\mu, \Delta)}] + \frac{1}{2\alpha^2[1 + (\omega^*/\alpha)^2]^{1/2}} + \frac{T(0)\gamma}{4\omega^*} \times (\pi/\beta)^{1/2}\,\mathrm{erf}(\omega^*/2\sqrt{\beta})\right\}, \quad (29)$$

where $\Sigma = N\pi a_0^2(\mu + 1)(\mu + 2)/\mu^2$, $\Delta = \mu\omega^*/2\rho_0$, $\gamma = (1 + 4\chi\rho_0/\mu)^{-(\mu+3)}$, and $P(n, y)$, is the incomplete gamma function.[12]

The proposed solution gives an ample scope for the study of the effect of the medium's microstructure on image degradation during image transfer through fogs and clouds. Formula (29) for the gamma PSD is especially simple when μ is an integer, because in this case the incomplete gamma function $P(n, y)$ is[12]

$$P(n, y) = 1 - \exp(-y)\sum_{j=0}^{n-1}\frac{y^j}{j!}. \quad (30)$$

Figure 1 compares the OTF estimated through Eqs. (1) and (29) with the results of Monte Carlo calculations[5] combined with the Mie formulas to provide the single-scattering characteristics. Let us call such an algorithm the Monte Carlo–Mie method.

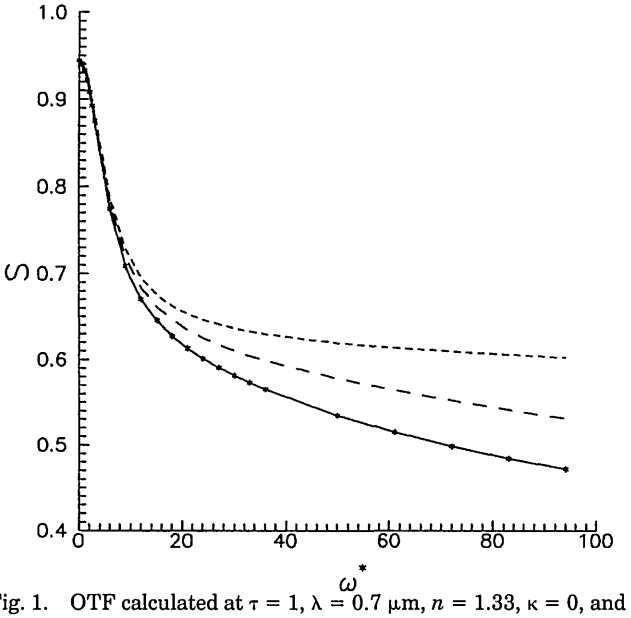

Fig. 1. OTF calculated at $\tau = 1$, $\lambda = 0.7$ μm, $n = 1.33$, $\kappa = 0$, and $\mu = 6$ based on the proposed Eqs. (1) and (29) for $a_0 = 4$ μm (solid curve), $a_0 = 8$ μm (long-dashed curve), and $a_0 = 50$ μm (short-dashed curve), and based on Monte Carlo calculations for $a_0 = 4$ μm (asterisks).

Here data are presented for a model[6] cloud C1, which is the gamma PSD with $\mu = 6$ and $a_0 = 4$ μm. As seen from Fig. 1, at $\tau = 1$ both methods give practically the same results for all ω^*. Figure 1 also shows the results of the calculations for polydispersion with large particles at $a_0 = 8$ μm and $a_0 = 50$ μm.

As seen from both Eq. (1) and Fig. 1, the function $D(\omega^*) = -\ln[S(\omega^*)/\tau]$ for nonabsorbing scattering media at small ω^* values does not practically depend on the mode radius a_0. It originates for two reasons: First, at $\chi = 0$ the geometrical optics phase function, $\eta_2(\omega^*)$, and $\eta_1(\omega^*)$ do not depend on a_0. Second, at $\omega^* \to 0$, the diffraction component $\eta_1(\omega^*)/\Sigma$ is proportional to the small value ρ_{21}^{-1} [see Eq. (15)]. On the contrary, at large ω^*, dependence of the function $D(\omega^*)$ on the mode radius is essential [see Eq. (16) and Fig. 1]. The parameter a_{32} of the PSD can be obtained through the OTF measurement.[13,14] Analysis of the data reveals that the OTF dependence on μ at a fixed value of $a_{32} = a_0(1 + 3/\mu)$ is rather poor,[13] and the a_{32} value is the most influential parameter of the microstructure relating to the OTF estimations.

Figure 2 gives the τ dependence of $F = -\ln[S(\omega^*, \tau)]$ for a few ω^* values. One can see that the values of the transmission coefficient, which is $S(\omega^* = 0, \tau)$, agree with the results obtained with the Monte Carlo–Mie method for all $\tau < 7$. Our simple approach ensures good accuracy, especially for low ($\omega^* \approx 0$) and high ($\omega^* \geq 50$) angular frequencies. The errors of our formula, which grow as τ increases, originate from the use of the SAA.

Figure 3 illustrates the OTF dependence on the microstructure parameters and the particle absorption. As seen from the figure, the OTF of the absorbing and scattering media shows a pronounced dependence on absorption at low frequencies.

We have demonstrated only the data for water aerosols. Image transfer through soil aerosols is also an important problem. Figure 4 gives the OTF for dust aerosols with $m = 1.53–0.008i$ and $\mu = 2$ at different mode radii of the PSD. Naturally, the OTF

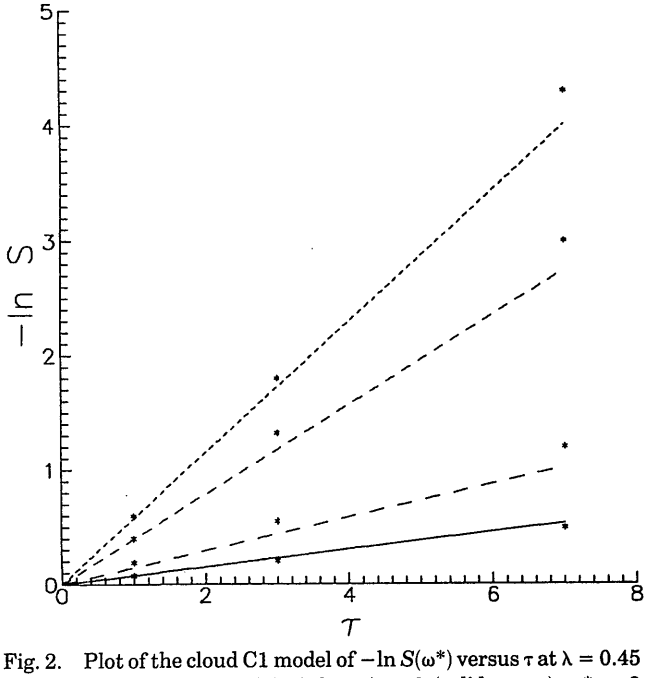

Fig. 2. Plot of the cloud C1 model of $-\ln S(\omega^*)$ versus τ at $\lambda = 0.45$ μm based on Eqs. (1) and (29) for $\omega^* = 0$ (solid curve), $\omega^* = 3$ (long-dashed curve), $\omega^* = 12$ (medium-dashed curve), and $\omega^* = 50$ (short-dashed curve), and on Monte Carlo calculations for the same values of ω (asterisks).

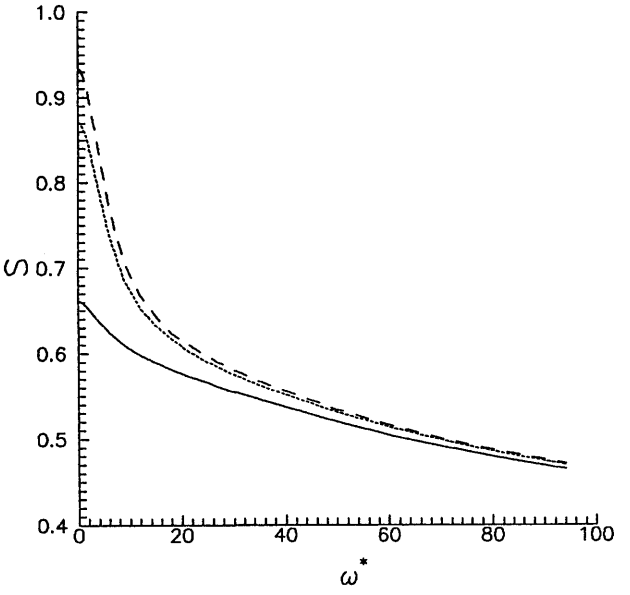

Fig. 3. OTF calculated with the proposed Eqs. (1) and (29) at $\tau = 1$, $\lambda = 0.7$ μm, $n = 1.33$, $\mu = 6$, and $a_0 = 4$ μm, for $x = 10^{-2}$ (solid curve), $\kappa = 10^{-3}$ (short-dashed curve), and $\kappa = 10^{-4}$ (long-dashed curve).

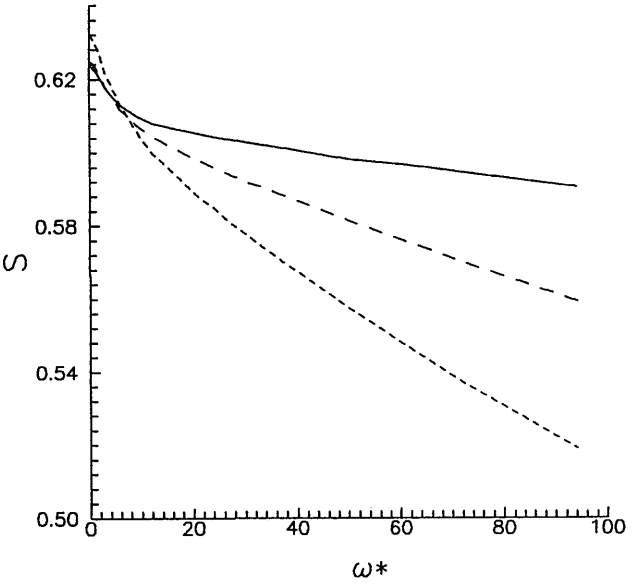

Fig. 4. OTF calculated with the proposed Eqs. (1) and (29) at $\tau = 1$, $\lambda = 0.7$ μm, $n = 1.53$, $\kappa = 0.008$, and $\mu = 2$ for $a_0 = 30$ μm (solid curve), $a_0 = 10$ μm (short-dashed curve), and $a_0 = 5$ μm (long-dashed curve).

value for dust aerosols is lower than that for water because of the strong light absorption in particles.

5. Conclusion

We have managed to directly relate the OTF to the particle-size distribution parameters and to the complex refractive index of the particles. To do so, we combined the special geometrical optics solution for optical parameters of particles and the small-angle solution for the OTF. The accuracy of the derived formulas appears to be high enough: the error of the OTF estimation is no more than 7% at $a_{32} > 10\lambda$ up to $\tau = 7$ for nonabsorbing particles, and it provides high accuracy at any τ for absorbing and scattering media. This approach is indispensable in the study of the effect of the microstructure on imaging through aerosols, clouds, and fogs and in the consideration of the OTF changes in the processes of condensation, coagulation, or evaporation of drops that are both natural and artificially stimulated.

The use of our OTF formula can save much time in comparison with conventional techniques such as the Mie calculations for optical particle parameters or the Monte Carlo calculations that provide OTF.

Relation (16) is the key to the inverse problem, and the parameter a_{32} of the PSD can easily be obtained through OTF measurements.[13,14] Such a method can be considered as a generalization of the small-angle method[15] of particle sizing that takes into account the multiple-scattering effect.

Appendix A

Here we give a convenient analytical approximation for the phase function $P(\theta)$ of polydispersions of large spherical particles

$$P(\theta) = \frac{4\pi N}{k^2\sigma}\int_0^\infty I(a,\theta)f(a)\mathrm{d}a, \quad \int_0^\infty f(a)\mathrm{d}a = 1. \quad \text{(A1)}$$

Here N is the number concentration, $k = 2\pi/\lambda$, λ is the wavelength, σ is the scattering coefficient, $I(a, \theta)$ is the dimensionless Mie intensity, and a is the particle radius.

It is known that the Mie calculation are the more cumbersome for particles with larger diffraction parameters $\rho = ka$. The geometrical optics approximation for $I(a, \theta)$ gives

$$I(a,\theta) = \sum_{j=1}^{\infty} I_j(a,\theta). \quad \text{(A2)}$$

Here $I_1(a, \theta)$ is the radiance of the Fraunhofer diffraction, $I_2(a, \theta)$ and $I_3(a, \theta)$ are, respectively, the radiance of the light reflected by the particle surface and that transmitted by the particle without any reflection inside the particle, with

$$I_1(a,\theta) = \frac{\rho^2 J_1^2(\rho\theta)}{\theta^2}$$

$$I_2(a,\theta) = \frac{\rho^2 R(\theta)}{4},$$

$$I_3(a,\theta) = \frac{\rho^2 T(\theta)}{4}\exp[-c\Delta(\theta)]. \quad \text{(A3)}$$

Here $J_1(\rho\theta)$ is the first-order Bessel function, $c = 4\chi\rho$ and

$$R(\theta) = \frac{1}{2}\sum_{j=1}^{2}\left[\frac{N_j^2(1-q^2)^{1/2} - (n^2-q^2)^{1/2}}{N_j^2(1-q^2)^{1/2} + (n^2-q^2)^{1/2}}\right]^2, \quad \text{(A4)}$$

$$T(\theta) = \left(\frac{2n}{n^2-1}\right)^4 \frac{(nq-1)^3(n-q)^3(1+q^4)}{2q^5(1+n^2-2nq)^2}, \quad \text{(A5)}$$

$$\Delta(\theta) = \frac{n-q}{(1+n^2-2nq)^{1/2}}, \qquad q = \cos\frac{\theta}{2},$$

$$N_1 = 1, \qquad N_2 = n^2. \quad \text{(A6)}$$

For any particle in the small-angle region, which is of interest in OTF investigations, and for all angles for absorbing particles, the terms in Eq. (A2) with $j > 3$ can be neglected.[7]

To simplify this result, we suggest using the following approximations:

$$R(\theta) = \exp(-\alpha\theta), \qquad T(\theta) = T(0)\exp(-\beta\theta^2 - c),$$

$$\Delta(\theta) = 1 - \frac{2n-1}{4(n-1)}\theta^2, \quad \text{(A7)}$$

where

$$T(0) = \frac{1}{(n-1)^2}\left(\frac{2n}{n+1}\right)^4, \quad \text{(A8)}$$

and the values of α and β depend only on the real part n of the complex refractive index (see Table 2). The error of approximation (A7) does not exceed 15% at $\theta < 35°$ and $n = 1.33$–1.6.

Thus, instead of Eqs. (A1)–(A6) we have

$$I(a,\theta) = \frac{\rho^2}{4}\sum_{j=1}^{3} q_j, \quad \text{(A9)}$$

Table 2. Values of α and β as Functions of the Real Part of the Refractive Index n

n	α	β
1.33	3.0	4.7
1.4	2.7	3.6
1.53	2.4	2.4
1.6	2.3	2.0

where

$$q_1 = \frac{4J_1^2(\theta\rho)}{\theta^2}, \qquad q_2 = \exp(-\alpha\theta),$$

$$q_3 = T(0)\exp(-\beta\theta^2 - c),$$

and

$$\sigma(\theta) = N\pi M_2 \times [D(\theta) + \exp(-\alpha\theta) + \gamma T(0)\exp(-\beta\theta^2 - c)], \tag{A10}$$

where

$$\gamma = M_2^*/M_2, \qquad M_2 = \int_0^\infty a^2 f(a)\mathrm{d}a,$$

$$M_2^* = \int_0^\infty a^2 \exp(-c)\mathrm{f}(a)\mathrm{d}a, \tag{A11}$$

$$D = \frac{4\int_0^\infty a^2 f(a)J_1^2(\theta\rho)\mathrm{d}a}{\theta^2\int_0^\infty a^2 f(a)\mathrm{d}a}, \qquad \sigma(\theta) = \sigma P(\theta). \tag{A12}$$

For the gamma particle-size distribution we have

$$M_2 = a_0^2\left(1 + \frac{1}{\mu}\right)\left(1 + \frac{2}{\mu}\right),$$

$$\gamma = \frac{1}{(1 + 4\chi\rho_0/\mu)^{\mu+3}}, \qquad \rho_0 = ka_0, \tag{A13}$$

$$D(\theta) = \left(\frac{\rho_0}{\mu}\right)\sum_{n=0}^{\infty}\frac{(-n)^n\Gamma(2n+3)\Gamma(2n+5+\mu)}{\Gamma(\mu+3)\Gamma^2(n+2)\Gamma(n+3)n!}\left(\frac{\theta\rho_0}{2\mu}\right)^{2n}. \tag{A14}$$

To obtain the last formula we use the known expansion[12] given by

$$J_1^2(z) = \left(\frac{z}{2}\right)^2\sum_{n=0}^{\infty}A_n z^{2n},$$

$$A_n = \frac{(-1)^n\Gamma(2n+3)}{4^n\Gamma^2(n+2)\Gamma(n+3)n!}. \tag{A15}$$

From Eq. (A10) at $\theta = 0$ we have

$$P(0) = \pi N M_2(\rho_0/\mu)^2(\mu+4)(\mu+3)/\sigma, \tag{A16}$$

where the geometrical optics components are neglected. As follows from Eq. (A16), for large nonabsorbing spheres when $\sigma = 2\pi N M_2$, we have

$$P(0) = (1 + 3/\mu)(1 + 4/\mu)\rho_0^2/2. \tag{A17}$$

Thus, at $\mu \to \infty$, $P(0) = \rho_0^2/2$, as would be expected.[7,8] Let us consider the known model[6] of cloud C1, which is the gamma distribution of water drops with $\mu = 6$ and $a_0 = 4$ μm. For cloud C1, from Eq. (A17) at $\lambda = 0.7$ μm we have $P(0) = 1611$. The Mie calculation[6] gives $P(0) = 1680$, and the discrepancy is approximately 4%. The accuracy of the simple phase function formula Eq. (A15) can be judged with Table 3, where the data of the Mie calculation and of the Eq. (A10) approximation are compared for the cloud C1 model at $\lambda = 0.7$ μm. The discrepancy reaches a value of 15% only at $\theta = 35°$ and is smaller for values of $\theta < 35°$. Naturally, the error of the proposed phase function approximation decreases with increasing particle radii and absorption.

Table 3. The Angular Scattering Coefficient $\sigma(\theta)$ (km^{-1}) for the Model Cloud C1 Provided by Mie Calculations[6] and Eq. (A10) with Relative Percent Discrepancies Δ

	$\sigma(\theta)$		
θ (deg)	Mie Theory	Eq. (A10)	Δ (%)
0	2.81×10^{-4}	2.53×10^{-4}	9.9
1	1.98×10^{-4}	1.77×10^{-4}	10.7
2	7.56×10^{-3}	7.05×10^{-3}	6.8
3	2.22×10^{-3}	2.16×10^{-3}	2.4
4	8.18×10^{-2}	8.06×10^{-2}	1.4
5	4.48×10^{-2}	4.38×10^{-2}	2.2
6	3.08×10^{-2}	3.01×10^{-2}	2.3
7	2.36×10^{-2}	2.33×10^{-2}	1.5
8	1.93×10^{-2}	1.93×10^{-2}	<1
9	1.66×10^{-2}	1.67×10^{-2}	<1
10	1.47×10^{-2}	1.49×10^{-2}	−1.4
15	9.78×10^{-1}	1.03×10^{-2}	−5.3
25	5.22×10^{-1}	5.42×10^{-1}	−3.7
35	2.74×10^{-1}	2.32×10^{-1}	15

References

1. E. P. Zege, A. P. Ivanov, and I. L. Katsev, *Image Transfer through a Scattering Medium* (Springer-Verlag, Berlin, 1991), Chap. 6, p. 186.
2. A. Ishimaru, *Wave Propagation and Scattering in Random Media* (Academic, New York, 1978), Vol. 2.
3. L. Bissonnette, "Imaging through fog and rain," Opt. Eng. **31,** 1045–1052 (1992).
4. P. Bruscaglioni, P. Donelli, A. Ismaelli, and G. Zaccanti, "Monte-Carlo calculations of modulation transfer function of an optical system operating in a turbid medium," Appl. Opt. **32,** 2813–2824 (1993).
5. A. S. Drofa and A. L. Usachev, "About vision in cloud medium," Izv. Akad. Nauk SSSR Fiz. Atmos. Okeana **16,** 933–938 (1980).
6. D. Deirmendjian, *Electromagnetic Scattering on Spherical Polydispersions* (Elsevier, New York, 1969).
7. K. S. Shifrin, "Scattering of light in a turbid medium," NASA Rep. TTF-447 (NASA, Washington, D.C., 1951).
8. W. J. Glantshing and S.-H. Chen, "Light scattering from water

droplets in the geometrical optics approximation," Appl. Opt. **20,** 2499–2509 (1981).
9. E. P. Zege and A. A. Kokhanovsky, "Integral characteristics of light scattering by large spherical particles," Izv. Akad. Nauk SSSR Fiz. Atmos. Okeana **24,** 695–701 (1987).
10. E. P. Zege and A. A. Kokhanovsky, *Extinction, Scattering and Absorption of Light by Spherical Particles* (Institute of Physics, Academy of Sciences of Belarus, Minsk, Belarus, 1992).
11. L. S. Dolin, "Light beam scattering in a turbid medium layer," Izv. Vyssh. Uchebn. Zaved. Radiofiz. **7,** 471–478 (1964).
12. F. Davis, "Gamma function and closed functions," in *Handbook of Mathematical Functions,* M. Abramowitz and I. A. Stegun, eds. (National Bureau of Standards, Washington, D.C., 1964), p. 80–118.
13. E. P. Zege and A. A. Kokhanovsky, "To determination of large particles sizes under multiple light scattering in a medium," Opt. Spektrosk. **72,** 220–226 (1991).
14. L. P. Volnistova and A. S. Drofa, "Quality of image transfer through a light scattering media," Opt. Spektrosk. **61,** 116–121 (1986).
15. K. S. Shifrin, *Introduction to Ocean Optics* (Gidrometeoizdat, Leningrad, 1983).